

7-1-2013

Inverted Linear Halbach Array for Separation of Magnetic Nanoparticles

Yumi Ijiri

Oberlin College, Yumi.Ijiri@oberlin.edu

Chetan Poudel

P. Stephen Williams

Lee R. Moore

Toru Orita

See next page for additional authors

Follow this and additional works at: https://digitalcommons.oberlin.edu/faculty_schol

Repository Citation

Yumi Ijiri, Chetan Poudel, P. Stephen Williams, Lee R. Moore, Toru Orita, and Maciej Zborowski. 2013. "Inverted Linear Halbach Array for Separation of Magnetic Nanoparticles." *IEEE Transactions on Magnetics* 49(7): 3449-3452.

This Article is brought to you for free and open access by Digital Commons at Oberlin. It has been accepted for inclusion in Faculty & Staff Scholarship by an authorized administrator of Digital Commons at Oberlin. For more information, please contact megan.mitchell@oberlin.edu.

Authors

Yumi Ijiri, Chetan Poudel, P. Stephen Williams, Lee R. Moore, Toru Orita, and Maciej Zborowski

Inverted Linear Halbach Array for Separation of Magnetic Nanoparticles

Yumi Ijiri¹, Chetan Poudel¹, P. Stephen Williams^{2,3}, Lee R. Moore², Toru Orita², and Maciej Zborowski²

¹Department of Physics and Astronomy, Oberlin College, Oberlin, OH 44074 USA

²Department of Biomedical Engineering, Lerner Research Institute, Cleveland Clinic, Cleveland, OH 44195 USA

³Cambrian Technologies, Inc., Cleveland, OH 44109 USA

A linear array of Nd-Fe-B magnets has been designed and constructed in an inverted Halbach configuration for use in separating magnetic nanoparticles. The array provides a large region of relatively low magnetic field, yet high magnetic field gradient in agreement with finite element modeling calculations. The magnet assembly has been combined with a flow channel for magnetic nanoparticle suspensions, such that for an appropriate distance away from the assembly, nanoparticles of higher moment aggregate and accumulate against the channel wall, with lower moment nanoparticles flowing unaffected. The device is demonstrated for iron oxide nanoparticles with diameters of ~ 5 and 20 nm. In comparison to other approaches, the inverted Halbach array is more amenable to modeling and to scaling up to preparative quantities of particles.

Index Terms—Magnetic liquids, magnetic separation, nanoparticles, permanent magnets.

I. INTRODUCTION

MAGNETIC nanoparticles are of much interest for a wide range of biomedical applications including hyperthermia, magnetic resonance imaging (MRI) contrast agents, magnetic particle imaging (MPI), and magnetic tagging and cell separation [1], [2]. In these applications, features such as device efficiency and resolution depend critically on uniformity, in not only the nanoparticle size, but also the nanoparticle magnetic properties such as magnetization and coercivity. Unfortunately, comparatively few purification methods have been developed to sort *nanoscale* materials on the basis of such features [3].

Many of the recent efforts to achieve magnetic nanoparticle separation stem from existing approaches for larger particles such as magnetic field-flow fractionation (MgFFF) [3], [4] and high gradient magnetic separation (HGMS) [5], [6]. In the modified methods, a variable field electromagnet preferentially retains larger, more magnetic nanoparticles, while smaller, less magnetic ones flow unimpeded. While these and other approaches [3] have yielded promising results, challenges remain in terms of getting higher throughput and characterizing better the separation process, given the particle interaction issues.

In this work, we describe a different method, in which a permanent magnet arrangement known as a Halbach array is used to provide the magnetic force necessary to separate magnetic nanoparticles. First proposed by Mallinson [7] and developed by Halbach to focus high energy particle accelerator beams [8], the arrangement involves modulating the magnetization vector of a series of magnets to create a high flux and low flux side. As described below, in contrast to most uses of this arrangement, we have designed and constructed a Halbach array in which the *low* flux side is used. The combination of a low field, yet high field gradient allows for separating disparate iron oxide nanoparticle suspensions.

Manuscript received October 28, 2012; accepted January 25, 2013. Date of current version July 15, 2013. Corresponding author: Y. Ijiri (e-mail: yumi.ijiri@oberlin.edu).

Color versions of one or more of the figures in this paper are available online at <http://ieeexplore.ieee.org>.

Digital Object Identifier 10.1109/TMAG.2013.2244577

II. MAGNETIC ARRAY DESIGN CONSIDERATIONS

A single domain, isolated magnetic nanoparticle of total magnetic moment \mathbf{m} in an inhomogeneous \mathbf{B} field experiences a magnetic force

$$\mathbf{F}_m = \nabla(\mathbf{m} \cdot \mathbf{B}). \quad (1)$$

For a nanoparticle in solution of viscosity η , this force may be opposed by a resulting Stokes' drag force of

$$\mathbf{F}_d = -3\pi\eta d_p \mathbf{v}_p \quad (2)$$

where d_p is the (hydrodynamic) diameter of the nanoparticle, and \mathbf{v}_p is its velocity. For

$$\mathbf{F}_d + \mathbf{F}_m = 0 \quad (3)$$

the particle achieves a steady state \mathbf{v}_p which, for sufficiently large \mathbf{m} and large gradient in field, may be sizeable enough to allow for separation of the particle in a MgFFF process.

As described previously [7], [8] and illustrated in Fig. 1, a linear (Halbach) arrangement of permanent magnets in which the magnetization vector rotates (typically by 90 degrees) from magnet to magnet creates a condition in which magnetic flux is concentrated on one side of the array over the other. This necessarily results in large gradients in field over single magnet arrangements [9] and in addition, creates fields and gradients that are substantially uniform on planes parallel to the array. Halbach arrays have recently been used to continuously sort micrometer-sized magnetic particles with a fluid channel placed over the high flux side of the array [10]. On the high flux side, the magnetic force in (1) is maximal, due to saturated large values of \mathbf{m} on the particles and the large field gradient.

However, for nanometer-sized magnetic particles, the moment per particle is significantly smaller, resulting in weaker separation forces. In addition, in moderate to high magnetic fields, the nanoparticles may chain or aggregate due to dipole-dipole interactions which can be characterized by an energy term

$$U_{dd} = \frac{\pi}{72} \frac{\mu_o M^2 d_m^6}{(d_m + 2\delta)^3} \quad (4)$$

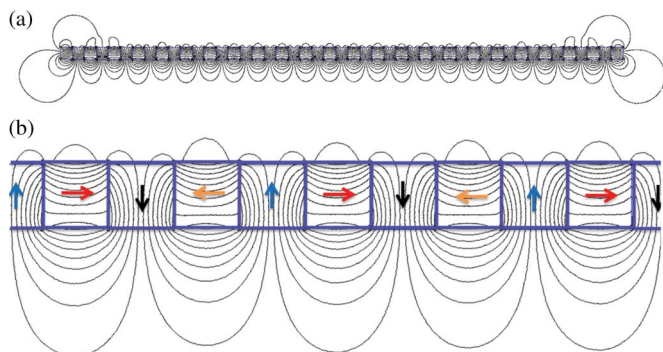


Fig. 1. (a) Simulated B field lines for a 47-magnet linear Halbach array of permanent magnets; neighboring magnets add to the flux on the bottom high flux side, but subtract on the top, low flux side. (b) Expanded view, showing the magnetization orientation for a section of nine complete magnets in the array. Field lines are ~ 0.02 T apart.

where the particles have magnetization values of M , magnetic diameter d_m and nonmagnetic coating thickness δ [11]. Note that the magnetic diameter d_m may be significantly different from the hydrodynamic diameter d_p , as the particles may have a sizeable portion that is not magnetic as a result of surface effects or more simply due to a surfactant coating. When U_{dd} becomes much greater than thermal fluctuations of order $k_B T$ (where k_B is Boltzmann's constant and T is temperature), a large distribution of clustered and chained nanoparticles may result, with other different-sized nanoparticles entangled inside, such that separation becomes even more challenging.

To address these issues, we have designed a linear Halbach array with a fluid channel across the low flux side of the assembly. The gradient of the magnetic field is still sizeable, but the magnetic field is modest to promote aggregation of only the most magnetic nanoparticles in a suspension, leading to more controllable separation of a mixture of nanoparticles.

III. DEVICE CONSTRUCTION AND PERFORMANCE

As shown in Fig. 2(a), an inverted Halbach array has been constructed with 47 nickel-plated Nd-Fe-B magnets (42 MGOe energy product, K&J Magnetics, Inc), each with dimensions of 0.64 cm (width) \times 0.64 cm (height) \times 5.08 cm (length) and magnetized through a 0.64 cm dimension. Across the array, the magnetization direction of each magnet is rotated by 90 degrees. The magnets are held in place with set screws and an aluminum frame, resulting in height variation from magnet to magnet of less than 5%. The array dimensions have been chosen to make use of readily obtainable magnets and other materials.

Fig. 2(b) depicts the flow channel for magnetic suspensions, constructed with a stainless steel base, a Viton rubber gasket, a borosilicate glass top plate, and a Plexiglas cover to allow for viewing of the fluid. The channel has dimensions of 23.3 cm (length) \times 1.27 cm (width) \times 0.025 cm (thickness), with an inlet to outlet distance of 22.9 cm. Materials have been chosen to allow for use with both aqueous and organic solutions. FEP Teflon tubing (0.08 cm inner diameter) has been used for the inlet and outlet, with magnetic suspensions injected or withdrawn using a syringe pump (Harvard Apparatus Syringe Pump 11 Elite). Additional stainless steel spacer plates are used to adjust the distance of the channel from the array.

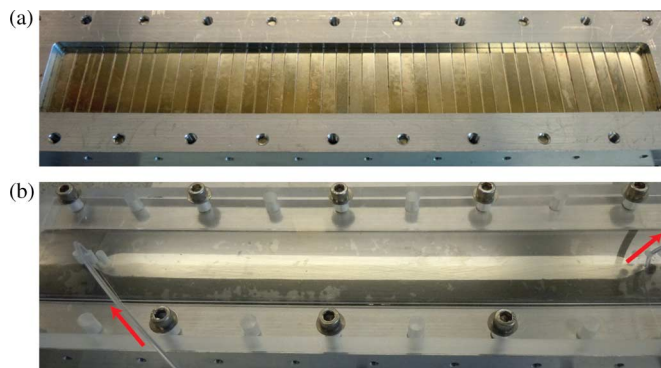


Fig. 2. (a) Photograph of the constructed Halbach array with low flux side on top. (b) Photograph with the flow channel placed on top of the array. Arrows indicate the tubing for inlet and outlet of magnetic fluid suspensions.

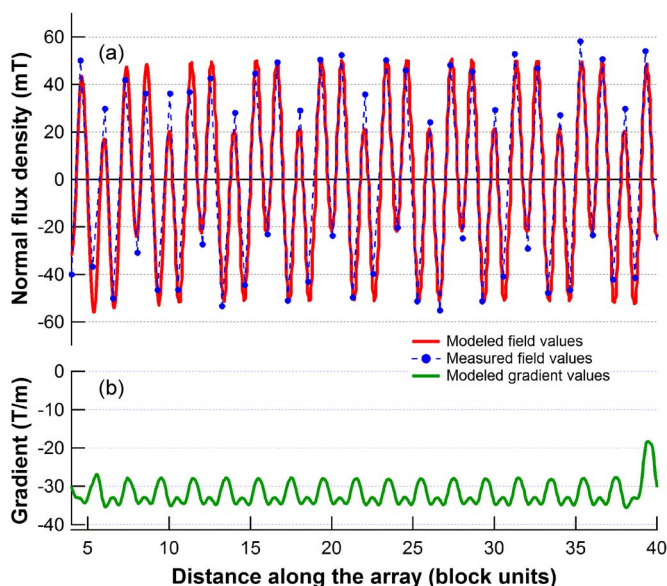


Fig. 3. (a) Plot of the normal component of the B field along the length of the magnet array at a distance 0.3 cm above the array (each block is 0.64 cm), as calculated from FEMMView (solid red) or measured with a gaussmeter probe (dashed blue). (b) Plot of the corresponding gradient of the field from FEMMView calculations.

The magnetic field of the assembly by itself has been determined with a Hall effect gaussmeter (Lakeshore) for several distances above the array. Fig. 3(a) shows the data for the normal component of the field measured at a distance of 0.3 cm from the magnet array, where the average $|B|$ field value is approximately 0.05 T. Also shown in the figure are the results of finite element method calculations performed with FEMM software, indicating the predicted field value in Fig. 3(a) and the gradient in Fig. 3(b), which has an average value of ~ 32 T/m [12]. There is good agreement between the measured and calculated values of the component of B, with the overall array uniformity high except near the ends where fringe effects occur. The flow channel location, width and length have been chosen to avoid these end effects.

As shown in Fig. 4, the average field and the field gradient depend on the distance from the array. Hence, the force on a suspension of nanoparticles as indicated in (1) can be adjusted by varying the distance of the channel from the magnet array,

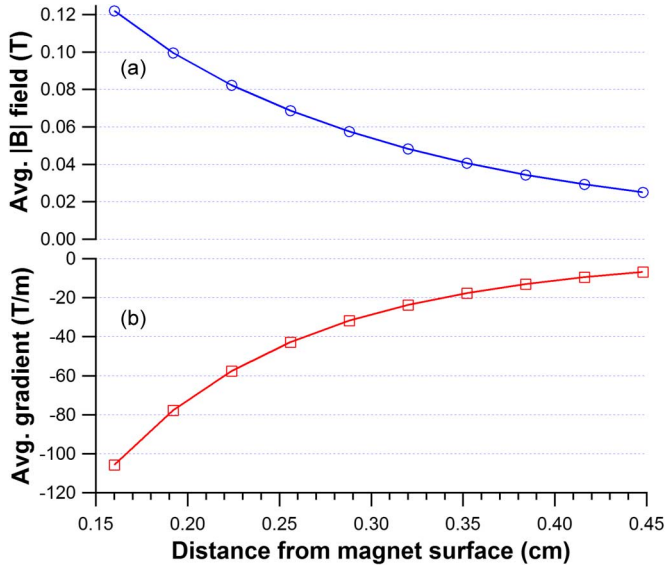


Fig. 4. Plot of the (a) averaged $|B|$ field and (b) gradient of B in the direction perpendicular to the surface of the magnet array as a function of distance above the array.

affecting both the gradient and the magnetization value for the particles.

The array has been tested with commercial iron oxide nanoparticles (Aldrich) of nominal sizes of 5 (± 1) and 20 (± 2) nm diameters with surfactant coatings of 1.5 nm, as determined from transmission electron microscopy (TEM). The particles are coated with oleic acid as surfactant and suspended in toluene with initial concentrations of 5 mg/mL. The particles' net moment as a function of applied magnetic field has been measured using a Lakeshore 7307 vibrating sample magnetometer (VSM), with the suspensions showing superparamagnetic-like behavior, with saturation values of $\sim 80\%$ and 90% of bulk magnetite for the 5 and 20 nm particles respectively.

From the size and moment information, we can then estimate the dipole-dipole energy from (4) for a specific value of applied magnetic field. For instance, in a B field of 0.05 T, we find the 5 nm diameter particles have U_{dd} of only 0.003 times that of room temperature thermal energy ($k_B T \sim 4.11 \times 10^{-21}$ J), whereas for the 20 nm diameter particles, U_{dd} is over 5 times greater than that associated with thermal motion. For one 5 nm and one 20 nm particle, the U_{dd} is still a small 0.08 times that of $k_B T$. Thus, it is reasonable to anticipate significant clustering of only the 20 nm diameter particles under this condition in contrast to the 5 nm ones.

Note that the steady-state velocity v_p of nanoparticles or clusters of nanoparticles can be projected from (3), given information on the effective particle diameter d_p , the fluid viscosity, the moment, and field gradient. Assuming for a cluster of 20 nm particles, a d_p of ~ 3 times the single particle diameter, a viscosity of toluene of 0.590 cP, and the moment and field values for the particles 0.3 cm from the magnet array, we estimate a v_p of $\sim 1 - 2 \mu\text{m/s}$. Since the flow channel thickness is 250 μm , the time for the clusters of 20 nm particles to traverse the channel width is $\sim 2-4$ minutes, which would suggest flow rates

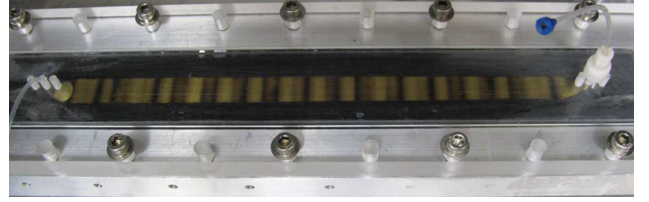


Fig. 5. Photograph of the device after a 50:50 by volume mixture of 5 and 20 nm particles has been passed through the flow channel. Prominent residue bands remain.

of under 0.2–0.4 mL/min to allow such clusters to deposit on the accumulation wall of the channel. Note that while the channel is oriented horizontally, settling of the clusters due to gravity is negligible, since the magnetic force F_m is several orders of magnitude greater than that due to gravity.

To explicitly test the performance of the constructed device, we have investigated its use with three separate suspensions containing 5 nm particles, 20 nm particles, and a 50:50 by volume ratio of 5 and 20 nm particles. The base of the channel has been set at a distance of 0.3 cm from the magnet array surface, with a 0.1 mL/min flow rate. While the 5 nm particle suspension passes through the channel leaving little visible sign of particles against the accumulation wall, the 20 nm particle suspension leads to a darkened residue. Similarly, as depicted in Fig. 5, upon sending the mixture through the channel, we observe significant banding, indicating depositing of nanoparticles, particularly the larger ones.

To quantify the degree of separation, small angle x-ray scattering (SAXS) measurements have been performed on the nanoparticle suspensions in transmission geometry using a Rigaku Ultima IV x-ray diffractometer (with a sealed tube copper $K\alpha$ source) with a liquid stainless steel sample holder of Kapton windows. The SAXS measurements were taken from 0.1 to 3.6 degrees 2θ with a step size of 0.02 degrees and a count rate of 1 minute per point.

As shown in Fig. 6, SAXS measurements of the unmixed solutions clearly indicate differences in the form factor beating as expected for nanoparticles of different diameters (patterns a and d). The mixture of the two (pattern c) displays an intermediate pattern. Passing this mixture over the array leads to a significant change in small angle scattering of the analyte (pattern b), resulting in a suspension more similar to that of the 5 nm particles (pattern a). The solid lines in Fig. 6 indicate fits to the SAXS data using the Rigaku NANO-Solver program [13]. From the fit data, it is found that the volume fraction ratio for the sorted suspension is now at 80%/20% for the small to larger particles vs. the initial mixture. Further work is necessary to determine what controls the sort ratio.

IV. CONCLUSION

We have demonstrated a novel method for separating suspensions of magnetic nanoparticles, based on their size and magnetic moments. As illustrated in Fig. 3, the magnetic characteristics of the magnet assembly agree well with finite element methods and thus allow for accurate modeling of magnetic forces. The device can separate suspensions of magnetic

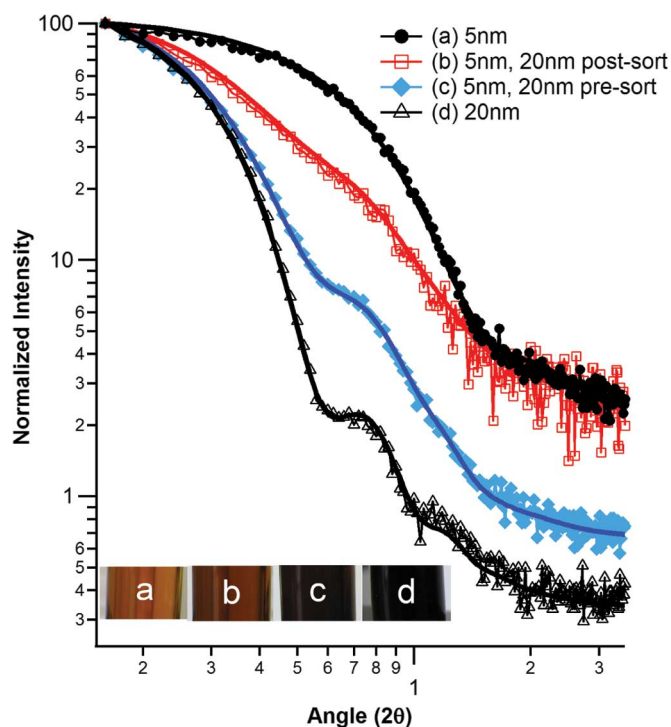


Fig. 6. SAXS measurements of intensity vs. 2θ angle for the a) 5 nm suspension, b) 5 and 20 nm mixture after sorting through the array c) 5 and 20 nm mixture before sorting through the array, and d) 20 nm suspension. Inset shows color of four fluids. Solid lines are fits to the SAXS data using the Rigaku NANO-Solver program.

nanoparticles in the 5 to 20 nm size regime. In addition, the planar geometry of the array is potentially scalable to much larger sizes, easily increasing throughput—an important concern in nanoparticle separation devices. It could also be made in a scaled-down microfluidics version.

Work is ongoing in order to optimize efficiency and speed of the sorting process based on considerations of the array profile and the expected degree of agglomeration for particles of different sizes and moment values.

ACKNOWLEDGMENT

This work was supported in part by the National Science Foundation (NSF) DMR-1104489, the National Institutes of

Health (NIH) CA62349, a Great Lakes College Association New Directions Initiative Award, the Cleveland Clinic, and an Oberlin College Research Status Award. The research made use of equipment obtained from NSF DMR-0922588 and DUE-9950606. The Visiting Scholar support to T. Orita was provided by Mie University, Japan. The authors also acknowledge B. Marton for his work in machining the array prototype.

REFERENCES

- [1] K. M. Krishnan, "Biomedical nanomagnetism: A spin through possibilities in imaging, diagnostics, and therapy," *IEEE Trans. Magn.*, vol. 46, pp. 2523–2558, 2010.
- [2] Q. A. Pankhurst, N. T. K. Thanh, S. K. Jones, and J. Dobson, "Progress in applications of magnetic nanoparticles in biomedicine," *J. Phys. D: Appl. Phys.*, vol. 42, pp. 224001-1–224001-15, 2009.
- [3] J. R. Stephens, J. S. Beveridge, and M. E. Williams, "Analytical methods for separating and isolating magnetic nanoparticles," *Phys. Chem. Chem. Phys.*, vol. 14, pp. 3280–3289, 2012.
- [4] P. S. Williams, F. Carpino, and M. Zborowski, "Magnetic nanoparticle drug carriers and their study by quadrupole magnetic field-flow fractionation," *Mol. Pharmaceutics*, vol. 6, pp. 1290–1306, 2011.
- [5] C. T. Yavuz, J. T. Mayo, W. W. Yu, A. Prakash, J. C. Falkner, S. Yean, L. Cong, H. J. Shipley, A. Kan, M. Tomson, D. Natelson, and V. L. Colvin, "Low field magnetic separation of monodisperse Fe_3O_4 nanocrystals," *Science*, vol. 314, pp. 964–967, 2006.
- [6] J. T. Mayo, S. S. Lee, C. T. Yavuz, W. W. Yu, A. Prakash, J. C. Falkner, and V. L. Colvin, "A multiplexed separation of iron oxide nanocrystals using variable magnetic fields," *Nanoscale*, vol. 3, pp. 4560–4563, 2011.
- [7] J. C. Mallinson, "One-sided fluxes—a magnetic curiosity," *IEEE Trans. Magn.*, vol. 9, pp. 678–682, 1973.
- [8] K. Halbach, "Design of permanent multipole magnets with oriented rare earth cobalt material," *Nucl. Instr. Meth.*, vol. 169, pp. 1–10, 1980.
- [9] M. E. Hayden and U. O. Häfeli, "'Magnetic bandages' for targeted delivery of therapeutic agents," *J. Phys.: Condens. Matter*, vol. 18, pp. S2877–S2891, 2006.
- [10] M. Hoyos, L. Moore, P. S. Williams, and M. Zborowski, "The use of a linear Halbach array with a step-SPLITT channel for continuous sorting of magnetic species," *J. Magn. Magn. Matl.*, vol. 323, pp. 1384–1388, 2011.
- [11] R. E. Rosensweig, *Ferrohydrodynamics*. New York: Dover Publications, 1997.
- [12] D. C. Meeker, Finite Element Method Magnetics ver. 4.0.1, (03Dec2006 Build), <http://www.femm.info> for description of approach to solve two dimensional planar electromagnetic problems.
- [13] Rigaku Corp. [Online]. Available: <http://www.rigaku.com/service/software/nanosolver>